Improving discrete particle packing models for the microstructural formation simulation of Portland cement

Mingzhi Wang[a,*], Abir Al-Tabbaa[b], Wei Wang[c]

a. School of Civil Engineering, Harbin Institute of Technology, 150006, CN

b. Department of Engineering, University of Cambridge, CB2 1PZ, UK

c. School of Civil Engineering, Harbin Institute of Technology, 150006, CN

*Corresponding author at School of Civil Engineering, Harbin Institute of Technology, 150006, CN

E-mail address: kevin18289@outlook.com

Abstract

The 3D solid phase spatial distribution strongly influences the electrical, mechanical and chemical properties of Portland cement microstructure. The commonly applied random sequential addition (RSA) method in cement microstructure formation simulation is causing over-computation of volume expansion due to the unrealistic initial geometry condition. However, it is difficult to search for a suitable model to represent the initial 3D pore structure with sufficient pore density range and compatibility with existing 3D cement microstructure models. An approach is proposed based on introducing a pseudo-contact mechanics analysis step to the RSA-discrete particle packing simulation scheme. The key control parameter to obtained specific pore density is identified to be the coefficient of friction after adjusting relative velocity distribution, lattice elastic constant and particle/domain size ratio. The proposed method enables the generation of random 3D pore structure with the same lattice configuration of major discrete cement microstructure formation models and Lattice Boltzmann Method (LBM), allowing more realistic 3D structure input and coupled modelling.

1. Introduction

The problem of particle packing has been studied intensively for decades both experimentally [1,2] and numerically [3-19]. In terms of mono-sized sphere packing, it was mathematically proved that 0.74 is the highest packing fraction [20]. However, the random particle packing is unlike artificial placement and the highest packing fraction 0.74 hardly exists in practise. Random loose packing (RLP) is commonly defined as the stable packing

phenomenon with minimum packing fraction and random close packing (RCP) is commonly defined as the densest packing phenomenon formed by random particle packing without chemical reaction and deformation. Through the previous study, a packing fraction of around 0.55 and a coordination number of 5 were observed for monosized sphere packing [2-4,12,23] in the case of RLP. On the other hand, a packing fraction of 0.64 and a coordination number of 6 were determined [1,4, 13-15] in the case of RCP. From this point of view, packing fraction and coordination number are often used as the macroscopic parameters to determine the packing degree when a visual 3D pore structure is not directly available. In this paper, random pore structure with a packing fraction of 0.55 and 0.64 and the corresponding coordination numbers are referred to as RLP and RCP structure, respectively. The debate about a better definition of RLP can be noticed through the development of particle packing models regarding the cohesive control and frictional control [2,12,23]. It has been as well debated that no lower packing fraction limit exists for RLP[23]. As a result, the packing fraction value of 0.64 is a better-recognised validation than that of RLP. In fresh cement microstructure, monosized distribution is seldom observed and Rosin-Rammler function has been widely used to represent the particle size distribution of cement particles [40]. In terms of polydisperse spheres, the packing fraction was found to be a function of the standard deviation if log-normal particle size distribution (PSD) is applied [6].

The computer simulation of a porous structure made of particles can be realized with various algorithms. To name a few, random sequential addition (RSA) [16,17] algorithm provides a straightforward solution by sequentially adding pre-defined geometry at a random position and overlap is not allowed. However, the upper packing fraction limit of RSA is almost always lower than RLP. Particle growth algorithm [5] simulates the packing process by increasing the radius of point or sphere placed with RSA. The size of the individual particle is often not under control to achieve a dense pore structure. Overlapping-relocation algorithm [14, 15] adjusts the particle's position by assigning a movement opposite to its overlapping with the other particles. The domain size is not under control since the sample volume keeps expanding with this method. For the purpose of having a user-defined sample size and PSD, the following two algorithms are considered to be well-developed. DigiPac [8] and the related DigiDEM [21] and DigiCGP [22] provide

a reliable solution for the issue of arbitrary shape random particle packing in a discrete system. Discrete element method (DEM) [23-25,34,35], which is though not originally designed for the packing issue, emphasizes the particle inter-force during the packing process in a continuous system and the RLP-RCP packing result is as well close to the determined value.

One of the important issues that the particle packing aids to solve is the microstructure development simulation of cement-based material as the result of hydration [26-29]. These cement microstructure formation simulations require an initial 3D porous structure with specific sample size and PSD, which is generally generated by RSA simulation. However, it was experimentally observed that fresh bulk cement paste possesses a packing density within the range of 0.480-0.514 measured with dry packing method and the range of 0.622-0.703 measured with wet packing method [30,31], which are higher than the maximum packing density (≈ 0.4) provided with RSA [38]. The inconsistence of the initial packing fraction between simulation and experiments inevitably leads to the over-computation of the volume expansion when the final results consist. This vital problem of unrealistic initial spatial distribution of fresh cement particles became outstanding only after the development of experimental techniques of measuring packing density of fresh cement in 2008 [30,31]. In terms of system compatibility, CEMHYD3D series [26,27] applying cellular automaton (CA) in the discrete system are naturally compatible with discrete packing algorithms such as DigiPac series [8,21,22]. On the other hand, HYMOSTRUC/μic series [28,29] applying particle growth algorithm in the continues system are well compatible with continuous sphere algorithms such as DEM and the original sphere growth algorithm [5]. Data conversion can be applied to link the incompatible simulation systems between particle packing and cement microstructure formation but data distortion is inevitable from the discrete-continuous conversion or the other way around. In the analysis aspect of the 3D pore structure, the Lattice Boltzmann Method (LBM) has become a well-accepted tool to simulate diffusive fluid in cement pore structure [36]. Novel model applying LBM to simulate the microscale cement hydration has recently been initialized [41].

Through the author's reproduction of pre-existing discrete models and the available data [2,8,21,22], it was found that the random structure generated had a considerably lower

packing fraction than the RCP structure and the experimental measurement of fresh cement. As previously mentioned, the continuous-discrete data conversion from DEM results will inevitably cause the change of key properties such as porosity and water/cement ratio. On the other hand, the un-converted data is unable to perform a sub-particle scale simulation such as the dissolution of a specific part of a cement particle. As a result, it is necessary to improve pre-existing discrete models to generate a random 3D pore structure directly in the discrete system for a wider structure range and better adjustability. This paper presents the author's solution for the issue and it is believed that this work inclines with the research interest of the simulation of particle packing and cement microstructure in a discrete system.

2. Methodology

2.1 Pre-simulation data and optimization

Before the conduction of the simulation, PSD data is independently generated. For general comparison and validation purpose, monosized particles are initially discussed in this paper. User-specified PSD can be applied from experimental measurement of fresh cement microstructure. The Log-normal distribution and Weibull distribution are then applied as examples for abitary PSD input. Structural data as presented by Fig.1(b) are generated with individual particle's position, size and particle number information in this step.

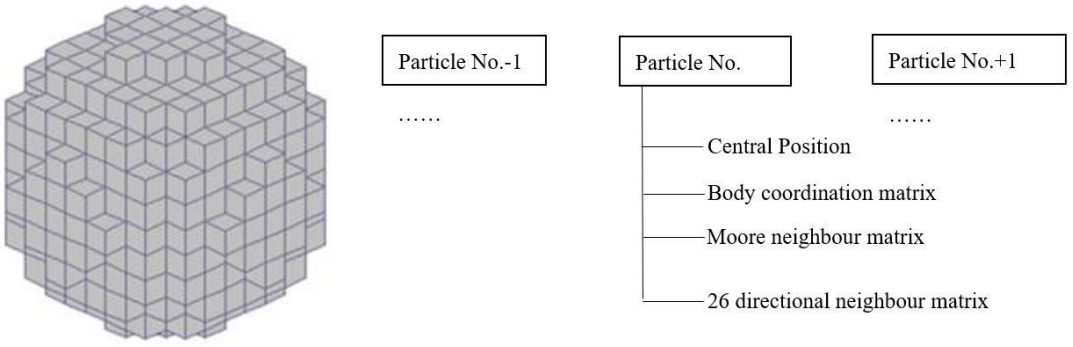

(a) (b)

Fig.1 (a)A digitized particle used in this model. (b) Structural data used in this model.

One voxel-based particle applied in this simulation is presented by Fig.1(a) which is in the same form with the common particle setting in the discrete packing system [8,21,22] and discrete cement microstructural formation system [26,27]. These particles are generated with Eq.1 in a 3D matrix.

$$X^2 + Y^2 + Z^2 = r^2 \quad (1)$$

where *X, Y* and *Z* is the coordination array for the particle with a size of *r*. The length mapping of the simulation was 1 μm per lattice (1 lu).

The calculation of each particle's body coordination matrix is time-consuming if it is conducted in the packing simulation. Optimization is therefore performed by pre-calculating the relative body coordination to the central coordination for a particle with a radius from 1 to 50 μm, so the body position update is directly conducted with the central position update during the packing simulation. Another optimization conducted is the pre-calculation of the 3D Moore neighbours of the body voxels and its 26 directional neighbours. The latter is obtained by performing a single lattice movement in one of the 26 discrete directions and then erasing the original body coordination. All the results of pre-calculation are stored in the particle structural data so that the contact check and movement assignment step in the packing simulation can be directly performed without real-time calculation.

2.2 Packing Simulation

Fig. 2(a) demonstrates the simulation flow of the programs. Periodic boundary condition is applied to the horizontal four directions and solid wall boundary condition is applied to the top and bottom direction of the 3D matrix named D1. The nature of the discrete system makes the direction of unit movement discrete as well, and 26 discrete directions are the maximum possible number for the 3D cubic lattice. The lattice system is named D3Q26 for 3D model with 26 possible movement directions following the naming principle of LBM. Initially, particles with pre-calculated PSD are placed into the 3D matrix with the RSA method. Then a contact analysis is conducted on each particle in its 6 orthogonal directions as illustrated by Fig.2 (b). In this simulation, contact is defined as the existence of the overlap between a particle and the Moore neighbours of the other particles. The movement in a certain direction is blocked if the contact analysis in this direction results in a true value (true=1).

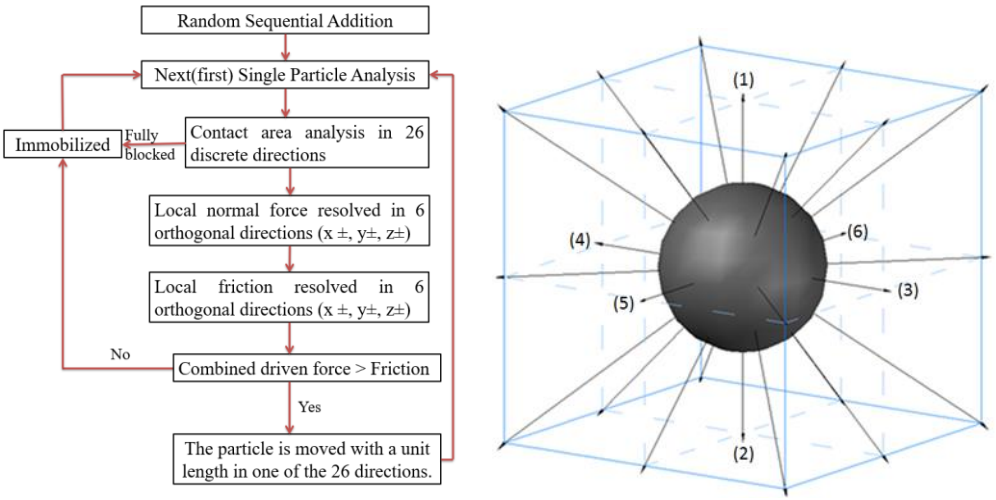

(a) (b)

Fig.2 (a)Simulation flow of this method. (b) Directions of contact analysis.

After the contact analysis step, a temporary 3D matrix named D2 is created. The Moore neighbours of all the particles are placed in D2 with the same central position. The overlap voxels in D2 caused by the increasing particle size are counted as the contact area *A* of the particles as shown in Fig.3(b), which is stored in the structural data during the calculation.

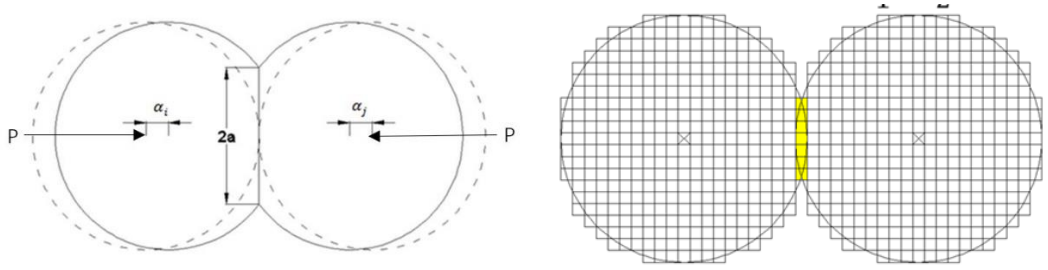

(a) (b)

Fig.3 (a)Parameters in contact analysis. (b) Contact area determination.

Then a pseudo-contact mechanics analysis is performed with Hertz repulsive force and the contact properties as shown with Eq.2 and Eq.3:

$$a = \left(\frac{3PR}{4E^*}\right)^{1/3} \quad (2)$$

$$\alpha_{ij} = \frac{a^2}{R} = \left(\frac{9P^2}{16RE^{*2}}\right)^{1/3} \quad (3)$$

where *a* is the radius of contact area; E^* is a constant relevant to the elastic modulus in the discrete system; 1/R is the equivalent contact curvature; α_{ij} is the relative displacement of the two centres, which is calculated as $\alpha_i + \alpha_j$. With equation (2) and (3), the following equation is derived:

$$P = \frac{4}{3} E^* a \alpha_{ij} \quad (4)$$

Assuming the contact area is a circle, the relation among normal force P, contact area A and relative displacement is obtained as given by Eq.5.

$$P = \frac{4}{3\sqrt{\pi}} E^* \sqrt{A} \alpha_{ij} = C_E \sqrt{A} \alpha_{ij} \quad (5)$$

where C_E is a general constant relevant to the elastic modulus. α_{ij} is treated as the relative velocities of one particle to its surrounding particles since each computation iteration is unit time, and the speed is calculated with Eq.6:

$$\alpha_{ij,k}/\Delta t = \sqrt{v_k^2} \quad k = 1,2,\dots,6 \quad (6)$$

where $\alpha_{ij,k}$ is the relative displacement of one particle in *kth* direction, *k* indicates one of the six orthogonal movement directions, Δt is the time mapping of the simulation, v_k is randomly assigned following a normal distribution with a mean of 0 and a standard deviation of s_v. As a result, thousands of $\alpha_{ij,k}/\Delta t$ values are directly assigned following Maxwell–Boltzmann distribution for the continues calculation of normal repulsive force in this discrete system. Friction threshold in the tangential direction for each particle is then calculated as given by Eq.7.

$$f = \mu P \quad (7)$$

where μ is the discrete coefficient of friction(*cof*). In this study, *cof* is the major adjustable parameter to control the density of the final packed structure.

Besides the local particle interaction, global influences such as gravity and vibration are also introduced as a universal force to all the particles, where the direction of gravity is downwards and the direction of vibration is randomly chosen in one of the four horizontal directions. The vibration is not emphasized in the work presented in this paper since it was experimentally proved that vibration intensity and frequency is not critical in the formation of the packed structure [1], which is also observed from this simulation. The above contact mechanics analysis step differs from 'real' contact mechanics calculation in the continuous system since the velocity map is not updated accordingly due to the built-in limitation of the discrete system.

With the conduction of the pseudo contact mechanics analysis, the resultant of forces $\vec{F}$ for each individual particle is obtained. A movement update step is then performed in D1.

This D3Q26 system only allows a single lattice movement in one of the 26 directions per iteration. The movement direction with the maximum vector scalar product calculation result given by Eq. 8 is determined to be the movement update direction.

$$R_i = \vec{F} \cdot \vec{n_i} \qquad i = 1, \ldots, 26 \tag{8}$$

where R_i is the scalar product in *i*th direction, $\vec{F}$ is the resultant of force vector on individual particle and $\vec{n_i}$ is the unit vector in *i*th direction. After the movement update, the previously designed procedure is repeated until a stable pore structure is formed. With the above design, no residual overlap exists in D1 and D2 makes use of the overlaps for the contact area calculation.

The method described above present an effort to bring the merits of pre-existing algorithms together in order to provide a reliable particle packing simulation directly in the discrete system. It applies the RSA method as the initial condition. The lattice configuration and sphere-like particle are compatible with CEMHYD3D, DigiPac series and D3Q27 LBM. The contact mechanics formula follows the Hertzian principal in DEM [34,35], which is fully functional off-lattice. The alternative contact area determination method and statistically determined relative velocity distribution in contact analysis are originally proposed to settle the problem between discrete and continuous system. Multi-task is conducted using parallel computation and packing result of this model is discussed in section 3.

2.3 Analysis methods

Packing fraction is obtained as the ratio of occupied voxels to the overall number of voxels. The porosity is directly obtained as the ratio of void voxels to the overall number of voxels. The coordination number for each particle is obtained by conducting a single step contact check of the overlaps between the Moore neighbour voxels of an individual particle in the D2 and the body voxels of the rest particles in the D1. Representative elementary volume (REV) analysis is conducted by the extracting samples with increasing sample size from the final packed structure in the D1 and chi-square criterion is applied as given by Eq.9 [37].

$$\chi^2 = \sum_{i=1}^{n} \frac{(p_i - \langle p \rangle)^2}{\langle p \rangle} \tag{9}$$

where χ^2 is the chi-square coefficient, p_i is the porosity of the extracted sample, $< p >$ is the average value of p_i, n=8 is the amount of extracted samples. In this study, A chi-square coefficient lower than 0.03% is applied as the criterion of REV determination and a cubic volume is then extracted to represent the structure.

2.4 Particle size distribution (PSD)

Simulation with mono-sized PSD is initially conducted to compare with well-recognized results from previous study of mono-sized particle packing. Rosin-Rammler function (Weibull distribution) [40] and log-normal distribution are applied for the polydisperse simulation to demonstrate the more practically simulated initial cement microstructure than previous model [38]. Eq. 10 and Eq. 11 gives the probability density function (PDF) of Weibull distribution and log-normal distribution, respectively.

$$PDF_{log-normal} = \frac{1}{x\sigma\sqrt{2\pi}} exp\ (-\frac{(lnr-\mu)^2}{2\sigma^2}) \quad (10)$$

$$PDF_{Weibull} = \frac{k}{\lambda}(\frac{r}{\lambda})^{k-1}\ e^{-(r/\lambda)^k} \quad (11)$$

where r is the radius of the particles, μ is the mean of log-normal distribution, σ^2 is the standard deviation of log-normal distribution, λ and k are the control parameters of Weibull distribution.

3. Results and Discussion

3.1 Visualized 3D porous structure

Fig.4 illustrates one visual result of the packing structure applying RSA, RLP and RCP with 500 discrete particles and 150×150 bottom area. The difference in the height of the packing structure can be intuitively observed. The fundamental aim of this research is to fully replace the 3D RSA input with a more realistic packed input for cement microscopic simulation with the consistency of macroscopic properties such as the volumetric ratio among solid phase, pores and fluid phase. Through reapply parametric study, s_v=3 and C_E=500 were found to be able to generate a sample with wider porosity range and better stability. In order to validate the presented simulation program with the well-recognized RCP phenomenon, parametric study and simulation were initially conducted with mono-sized spheres to observe whether 0.64 can be approached. In a mono-sized particle system, the difference in the size of the particle only influence the 3D resolution and the packing fraction result should be similar. Therefore, simulations were conducted with 5000 digitized spheres with radiuses of 8,9 and 10 lu. The early reported DigiPac algorithm is reproduced when *cof*=0, C_E=0 and S_v=0.

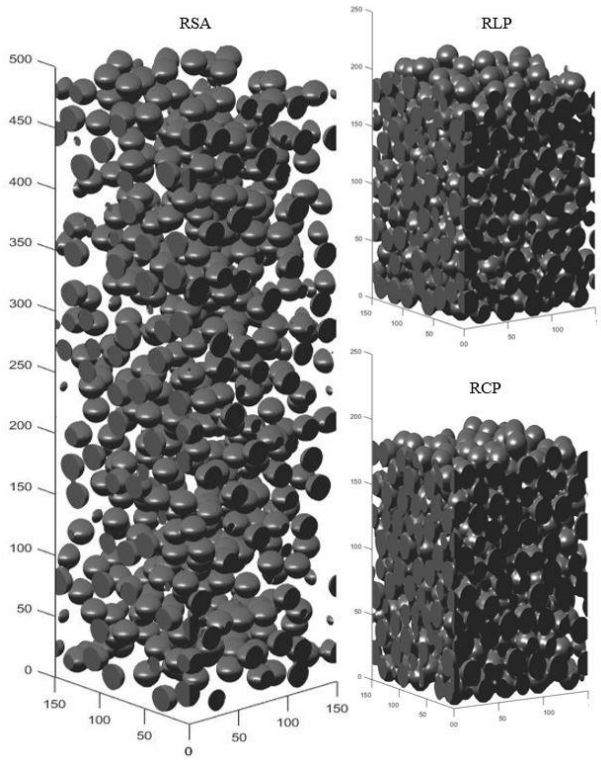

Fig.4 Three visual output from the model including RSA, RLP and RCP.

3.2 Sample volume determination with size ratio and REV analysis

Fig. 5 presents the packing fraction development under the influence of size ratio (L/d). L/d ratio is a parameter to describe the horizontal capacity of the domain to contain particles. It can be noticed from the figure that the frictionless packing reaches a packing fraction of around 0.64 when L/d>0, and the 0.64 is not much excessed afterwards. As a random particle placement process, a low L/d indicates a small horizontal area with a low possibility for particle placement. Such low possibility significantly influences the macroscopic porosity when the number of particles in this area is limited. When the number of the particle is high enough, the change of a few among becomes much less influential to the macroscopic parameter. In this study, it is suggested that L/d>20 should be adopted for the simulation with this method.

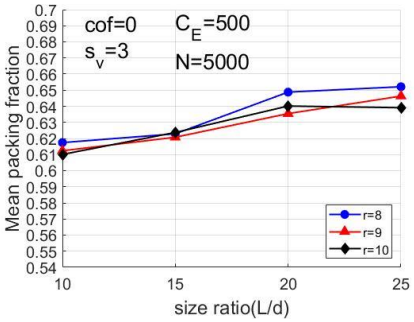

Fig.5 Influence of size ratio (L/d).

In a heterogeneous system, a small extraction from the whole sample may not be representative since such extraction could be a specific part of the sample. An extraction from the fresh cement model as presented in Fig.4 could have an overestimated void ratio if most of the extraction is void phase. A REV analysis with log-normal PSD is conducted in this section to determine the minimum representative sample volume on this model and RSA model. Fig.6 (a) presents the void ratio moving from non-representative zone to the representative zone with the increment of extraction size. In order to quantify the REV size, chi-square criterion is applied as presented in Fig.6 (b). It can be noticed that the REV sizes are within the size range provided by the L/d ratio of 20 as previously discussed. REV requirement increased with both the increment of the standard deviation (*sd*) of the PSD and *cof*, due to the enlarged particle size range and porosity, respectively. A comparison analysis is conducted on the RSA model with *sd*=0.25, and it can be noticed that the REV size requirement of the RSA model in the size determination range of (80,140). 140×140×140 is found to be a universal REV for all current digital samples.

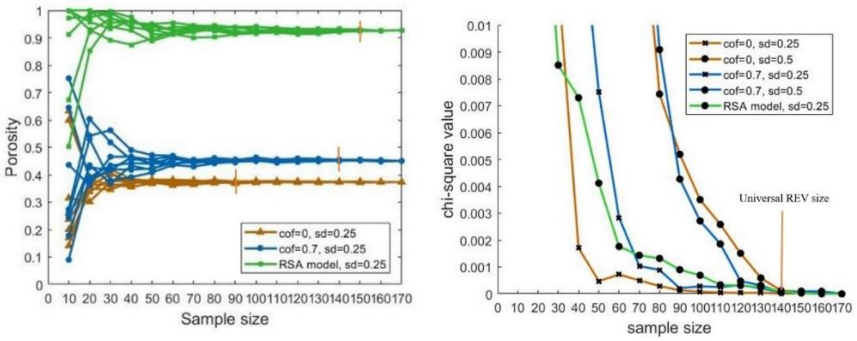

(a) (b)

Fig.6 (a) Void ratios of the extracted samples. (b)Chi-square value development in terms of the extraction size.

3.3 Mono-sized simulation and validation

Fig. 7 present the simulations to generate adjustable pore structures using the *cof* as the only tuning parameter. L/d=20, s_v=3 and C_E=500 are applied for the 5000 particles simulation. The dependence of particle size is minimised but not entirely removed. As a matter of fact, the voxelized particles applied both in this and previous discrete models is not in the same shape as spheres. Due to the meshing, some of the voxels in the sphere surface is not counted as part of the particle. As a result, the minimized dependence of radius is actually dependence of particle shape and it is impractical to pursuit a single curve for every particle size. The voxelization is essential for sub-particle modification for discrete cement microstructure formation simulation and analysis. In 3D discrete cement models, the matrix representing the particle body can be coupled with mass density matrix so that a single particle with heterogeneous density distribution can be simulated. Such heterogeneous density distribution is fundamental to simulate the surface mass lost during the dissolution of the solid phase. The same argument as well applied to the pore matrix with which a 3D fluid density distribution can be coupled. In this case, the voxelization process narrows the homogeneous assumption to the scale of a single voxel before the construction and solution of the extremely complicated, if not impossible, the 3D theoretical description of reactive cement microscopic system. It is as well argued that no purely continuous simulation exists if the fundamental calculation is conducted in a binary system such as modern computers, where there only 0 and 1 and nothing in-between.

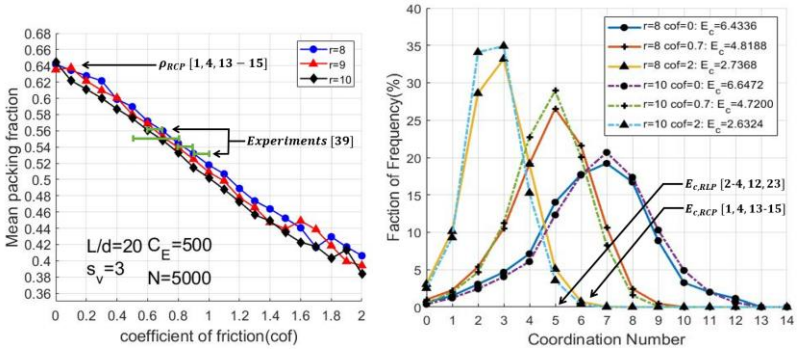

(a) (b)

Fig.7 Different pore structure generated with a varying coefficient of friction: (a) Extracted packing fraction development. (b) Extracted coordination number distribution.

Fig. 7(a) presents the packing fraction of the simulated 3D pore structure in terms of the *cof* changes. The behaviour of loose pore structure formation under increased interparticle

friction is quantitatively simulated in the discrete system. At the point of *cof*=0.7, a packing fraction of 0.55 is obtained. Fig. 7(b) presents the coordination number distribution when *cof* equals 0, 0.7 and 2, respectively. E_c denotes the mean coordination number in the figure. The study shows that the packed structure simulated with this method has an $E_c \approx 6.4$ when the packing fraction is around 0.64 and an $E_c \approx 4.7$ when the packing fraction is around 0.55. In this studied, the stable structure is defined as the status packing fraction change is within 0.01% where most of the particles are immobilized. The existence of the pore structure with a packing fraction lower than 0.55 supports the argument that 0.55 is not the bottom limit of the RLP. However, *cof*=0.7 is still used to generated loose pore structure in the polydisperse simulation as discussed in section 3.5.

3.4 Comparison simulation

A comparison simulation without the pseudo contact mechanics analysis step is presented by Fig.8(a) with solid wall boundary condition applied at the bottom. A noticeable improvement in the highest packing fraction, which is very close to 0.64, can be observed as the direct result of the introduction of the pseudo contact mechanics analysis step proposed in this paper. In the comparison study, r=9 lu, L/d=20 and REV size of the sample are applied. As previously discussed, the range of dimensionless particle size does not significant influence the representativity of a numerical test when the size/domain ratio is fixed since mono-sized particle packing is independent of the particle size. In terms of hardware requirement, single non-parallel computation from RSA to a stable structure made of 6000 particles in 400×400×2300 matrix takes Intel(R) Xeon(R) CPU E5-1630 9482s to complete, with a peak RAM demand of 3 GB and 10% CPU occupation. The introduction of the pseudo contact mechanics analysis step increased the computation time by 20.6% with the same program setting. The proposed algorithm can be implied in the previously mentioned models for different performance without amending the simulation framework. Fig.8(b) presents the simulation result of the proposed algorithm and the increment of the maximum packing fraction is demonstrated. The increment is necessary because the experimental measurement of the packing fraction of fresh cement process higher limits than previous discrete packing model, and the RSA model applied in previous cement hydration simulation.

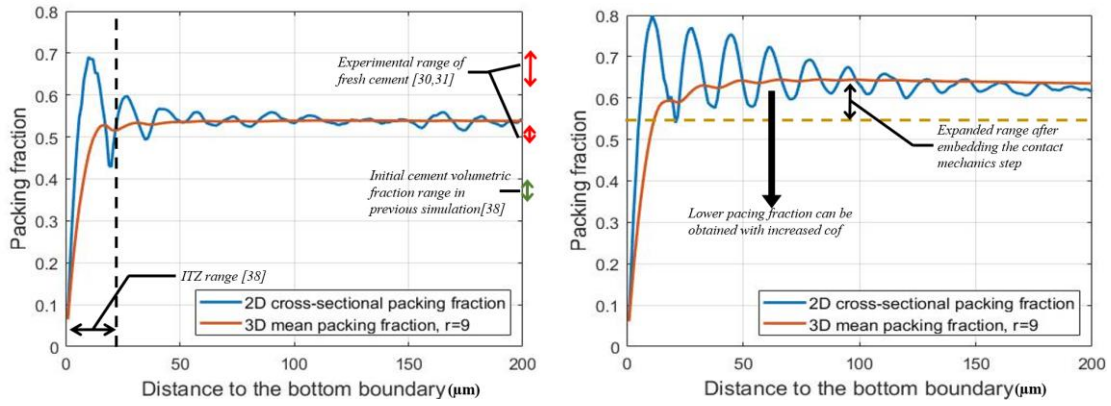

(a) (b)

Fig.8 (a) Simulation without the contact mechanics step. (b)Simulation including contact mechanics step.

One noticeable packing behaviour related to the cement microstructure is that the porosity is increased when the measurement 2D cross-section is closer to the bottom boundary. This behaviour corresponding well to the original of the ITZ between bulk cement paste and aggregates as a result of the wall effect. The ITZ thickness simulated with this comparison simulation is 20μm. It needs to be mentioned that properties such as ITZ thickness, porosity and coordination number are extracted from the more important random 3D structural data. The traditional RSA can also reproduce this phenomenon to some extent, but the porosity is significantly higher than prastical value. Embedding particle packing model can solve this vital problem of unrealistic intial input to some extend, and this work presents a further improvement of a suitable packing algrithm by extending the maximum packing fraction limit.

3.5 Polydisperse simulation

Monosized particles are seldom observed in fresh cement paste. Simulations are conducted in this section to model the fresh Portland cement sample with cement particles following log-normal distribution and Weibull distribution as presented in Fig.9. In log-normal distributed PSD, the mean particle radius is set to be the commonly applied 8μm and the coefficient of friction is set to be within the range of (0,0.7). The pre-hydrated cement particles are assumed to be digitized spheres. In practice, microscale PSD can be artificially tuned with fundamental methods such as sieving so that the requirement for the modelling work is actually the ability to have arbitrary PSD input.

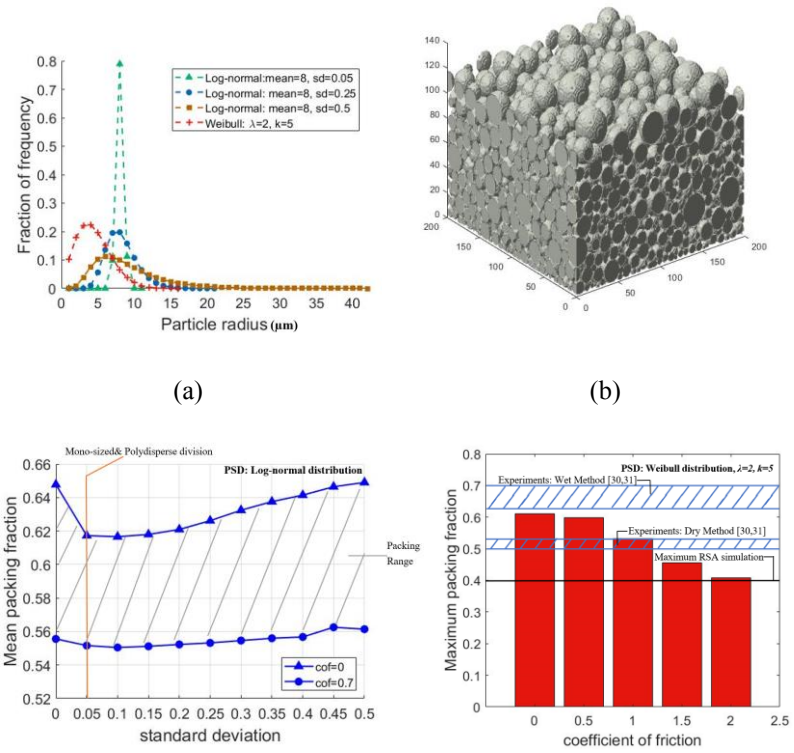

Fig.9 (a) Polydisperse PSD applied in the simulation. (b) Visualized result of the polydisperse simulation. (c) Simulation result with log-normal distribution. (d)Simulation result with Weibull distribution.

It can be noticed from Fig.9(c) that the packing fraction of simulated cement paste appears to be a function of the PSD standard deviation. The increment of the particle density caused by applying PSD is due to the fact that smaller particles can fill the pore made of bigger particles. When the standard deviation is low, the actual PSD in a continuous system is better graded than that in a discrete system, which is presented by the markers in Fig.9(a), because there is no limitation of the resolution. This limitation can be reduced through the application of higher resolution such as using r=16 to represent the 8μm cement particles. Higher resolution increases the amount of the available particle sizes, which has the same effect as increasing the PSD standard deviation with dimensionless consideration. Another common method is to increase the standard deviation to obtain a better grade as presented in Fig.9(a). In terms of cement particles, particles with radius significantly larger than the mean radius are often observed, indicating that low standard deviation may not apply to cement particles. In this study, the largest pre-calculated particles applied is r=54μm when the standard deviation reaches 0.65. When the standard deviation is above 0.1, the discrete

simulation result shows that the particle density increases with the standard deviation, which is the same as the continuous simulation. The results indicate that a higher resolution is required for the model when PSD of cement particles has a very low standard deviation, at the cost of increased computation demand. This simulation also presents that some macroscopic parameters of cement past such as void ratio is insufficient to represent the microscopic properties since different microstructures can offer the same macroscopic parameter. The shaded area indicates that the pore range provided by the method is (0.53,0.65) when *cof* is within (1, 0.7), corresponding to a void ratio range of (0.35,0.47). In the simulation with Weibull distribution, the result demonstrates an overlapping range with the experimental measurement using dry method [30,31]. Further simulation with the exact PSD of the fresh cement requires more determined experimental techniques to meaure the packing density and microscale PSD , which is unfoundatly not widely availiable.

3.6 Implement in discreet cement microstructural simulation

The previous simulations bring out the discussion of the necessity of this work. 3D Hydration models require a 3D pore structure of the fresh cement matching the experimental observation as the input. Initial properties such as void ratio, w/c ratio are calculated from the three-demensionally distributed solid phase, void phase and fluid phase. The commonly adopted RSA method and the original model without the pseudo contact mechanics analysis step presents a limitation in terms of the available porosity range and a lack of the porosity control. With the presented model, a 3D pore structure is generated with a wider density range and specific porosity can be generated using *cof* as the only control parameter. As an important branch of the cement microstructure formation simulation, discrete models have the ability to conduct sub-particle modification. Continuous-discrete conversion can provide input, but the microscopic changes of the particle surface will assemble to become a macroscopic difference in the initial properties. This problem is more severed if coupled modelling is conducted since the changes can assemble through thounds of iteration. The proposed discrete packing algorithm is fully compatible with discrete cement hydration model (CEMHYD3D and so on). The above discussion also applies to the LBM simulation of fluid in porous media, which is as well a part of research interest in the cementitious material since LBM is the upgrade of the

random walk algorithm widely applied in CEMHYD3D. The particles growth behavior in HYMOSTRUC can as well be reproduced with a well-constructed LBM simulation as presented in Fig.10 (b).

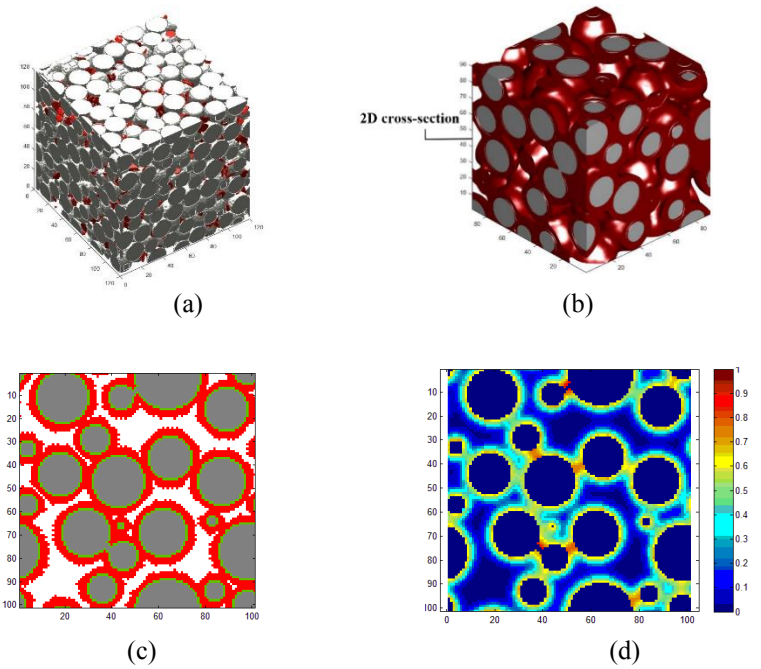

Fig.10 (a) Simulation with spheres and plates. (b) 3D particle growth behavior from the initial condition generated with this model. (c) 2D cross-section of the 3D structure. (d) LBM simulation of cement hydration with structure generated with this model.

Due to the same lattice configuration, the 3D pore structure generated with the proposed method can be directly embedded in the LBM simulation of diffusion behaviour in porous media (Fig.12(d)) and the discrete cement microstructural formation simulation (Fig. 10(b)) as geometry input. It can be noticed from Fig. 10 (d) that the geometry of a single particle become irregular during the cement hydration simulation, indicating a sub-particle modification on the heterogeneous distributed solid phase. In the voxelized system, each voxel of the particle can be amended according to the local diffusion-reaction mechanism. As a result, irregular hydration products with non-predefined shapes can be formed during the simulation.

Another advantage of the proposed packing algorithm is that it inherits the strong ability to simulate particle packing with arbitrary shape from the original discrete packing algorithm, which cannot be properly realized with current DEM. Modern experimental

cement system often contains non-spherical particles such as carbon black (plate-like), fibre (tube-like) in microscale and aggregates (arbitrary shape) in mesoscale. Fig.12(a) demonstrates a sphere-plate packing structure generated with this model as an example of fresh cement system containing non-sphere particles.

The packing density range provided by this model is 0.40-0.64. Though the highest packing density of 0.708 observed from the experiment on fresh cement is still not realized due to the lack of information on the PSD, considerable improvement has been made in terms of the density range and adjustability. Fluid density distribution can be assigned to the void phase matrix and solid mass density distribution can be assigned to the solid phase matrix both in macroscopic level or molecular level in order to perform the hydration simulation with the certain void ratio, w/c ratio, etc. In terms of volumetric w/c ratio, a packing density of 0.4 can result in a w/c ratio within the range of 0-1.5 and a packing density of 0.64 can result in a range of 0-0.5625 if the free water in the pore is the only consideration.

4. Summary

In this paper, a discrete particle packing algorithm is proposed to extend the maximum packing fraction to a value closer to experimental measurement of fresh cement. A pseudo contact mechanics analysis is introduced to enlarge the packing density range and the adjustability of the generated 3D pore structure. It was found that a local velocity distribution standard deviation of 3, a lattice elastic constant of 500 and an L/d ratio of above 20 is sufficient to be set as the fixed parameters in order to provide stable results with minimum size dependence. Coefficient of friction was applied as the only tuning parameter to obtain specific pore density. RCP packing fraction of around 0.64 was realized in the frictionless simulation. One RLP packing fraction of around 0.55 is realized when *cof*=0.7. Lower packing fraction was obtained with increased *cof*. Randomly assigned relative displacement following Maxwell–Boltzmann distribution is able to provide a packing fraction development matching previous experiment of frictional particle packing.

A comparison simulation was conducted to find that the introduction of the proposed pseudo contact mechanics analysis step indeed extends the packing density range. Single non-parallel computation from RSA to a stable structure made of 6000 particles in 400×400×2300 domain takes Intel(R) Xeon(R) CPU E5-1630 9482s to complete, with a

peak RAM demand of 3 GB and 10% CPU occupation. The introduction of the pseudo contact mechanics analysis step increased the computation time by 20.6% with the same program setting. Polydisperse simulation indicates that a resolution higher than 1μm per lattice is needed when the PSD standard deviation is lower than 0.1. Limitation of the discrete simulation on the available particle sizes still exists on the PSD assignment when the spherical assumption is applied.

The proposed packing model is in natural compatibility with discrete cement hydration simulation system and LBM system. Voxelization enables the hydration models to perform sub-particle modification as a result of the local diffusion-reaction mechanism. The strong ability to simulate particle packing with arbitrary shape is inherited from the original discrete packing algorithm. Though the highest packing density recorded in the experimental reports is still not reached, an improvement has been made for the discrete cement microstructure formation simulation with the expanded packing density range up to 0.64 and lower REV size requirement.

Conflict of interest

The authors declare that they have no conflict of interest.

References

[1] McGEARY, R. K. (1961) 'Mechanical Packing of Spherical Particles', *Journal of the American Ceramic Society*, 44(10), pp. 513–522.

[2] Onoda, G. Y. and Liniger, E. G. (1990) 'Random loose packing of uniform spheres and the dilatancy onset', 64(22), pp. 2727–2730.

[3] Song, C., Wang, P. and Makse, H. a (2008) 'A phase diagram for jammed matter', *Nature*, 453(7195), pp. 629–632.

[4] Valverde, J. M. and Castellanos, a (2007) 'Random loose packing of cohesive granular materials', *Europhysics Letters (EPL)*, 75(6), pp. 985–991.

[5] Lubachevsky, B. and Stillinger, F. (1990) 'Geometric Properties of Ran- dom Disk Packings', *Journal of statistical physics*, 60(5/6), pp. 561–583.

[6] Brouwers, H. (2006) 'Particle-size distribution and packing fraction of geometric random packings', *Physical Review E*, 74(3), p. 31309.

[7] a.B. Yu *et al.* (2003) 'Computer simulation of the packing of fine particles', *International Journal of Materials and Product Technology*, 19(3/4), p. 324.

[8] Byholm, T., Toivakka, M. and Westerholm, J. (2009) 'Effective packing of 3-dimensional voxel-based arbitrarily shaped particles', *Powder Technology*. Elsevier B.V., 196(2), pp. 139–146.

[9] Caulkin, R. *et al.* (2006) 'An investigation of packed columns using a digital packing

algorithm', *Computers & Chemical Engineering*, 30(6–7), pp. 1178–1188.
[10] Corwin, E. I. *et al.* (2010) 'Model for random packing of polydisperse frictionless spheres', *Soft Matter*, 6(13), p. 2949.
[11] Cundall, P. A. and Strack, O. D. L. (1980) 'A discrete numerical model for granular assemblies', *Géotechnique*, pp. 331–336.
[12] Farrell, G. R., Martini, K. M. and Menon, N. (2010) 'Loose packings of frictional spheres', *Soft Matter*, 6(13), p. 2925.
[13] a.C.J. de Korte and Brouwers, H. J. H. (2013) 'Random packing of digitized particles', *Powder Technology*, 233, pp. 319–324.
[14] He, D., Ekere, N. N. and Cai, L. (1999) 'Computer simulation of random packing of unequal particles.', *Physical review. E, Statistical physics, plasmas, fluids, and related interdisciplinary topics*, 60(6 Pt B), pp. 7098–7104.
[15] Jia, X. and Williams, R. . (2001) 'A packing algorithm for particles of arbitrary shapes', *Powder Technology*, 120(3), pp. 175–186.
[16] Williams, S. R. and Philipse, a P. (2003) 'Random packings of spheres and spherocylinders simulated by mechanical contraction.', *Physical review. E, Statistical, nonlinear, and soft matter physics*, 67(5 Pt 1), p. 51301.
[17] Xu, W. X. and Chen, H. S. (2012) 'Microstructural characterization of fresh cement paste via random packing of ellipsoidal cement particles', *Materials Characterization*, 66, pp. 16–23.
[18] Yang, R. Y. *et al.* (2007) 'Simulation of the packing of cohesive particles', *Computer Physics Communications*, 177(1–2 SPEC. ISS.), pp. 206–209.
[19] Corwin, E. I. *et al.* (2010) 'Model for random packing of polydisperse frictionless spheres', *Soft Matter*, 6(13), p. 2949.
[20] T. C. Hales, 'The status of the Kepler conjecture', *Math. Intelligencer,* 16, no. 3, (1994), 47–58.
[21] Caulkin, R. et al. (2015) 'Impact of shape representation schemes used in discrete element modelling of particle packing', Computers and Chemical Engineering. Pergamon, 76, pp. 160–169. doi: 10.1016/j.compchemeng.2015.02.015.
[22] Jia, X. *et al.* (2008) 'Property predictors for packed columns using Monte Carlo and Discrete element digital packing algorithms.pdf', *Computer Modeling in Enfineering and Sciences*, 23(2), pp. 117–125.
[23] Dong, K. *et al.* (2006) 'Role of Interparticle Forces in the Formation of Random Loose Packing', *Physical Review Letters*, 96(14), p. 145505.
[24] Powell, M. S. *et al.* (2011) 'DEM modelling of liner evolution and its influence on grinding rate in ball mills', *Minerals Engineering*. Elsevier Ltd, 24(3–4), pp. 341–351.
[25] Thakur, S. C., Ooi, J. Y. and Ahmadian, H. (2016) 'Scaling of discrete element model parameters for cohesionless and cohesive solid', *Powder Technology*. Elsevier B.V., 293, pp. 130–137.
[26] Bentz, D. P. (1997) 'Three-Dimensional Computer Simulation of Portland Cement Hydration and Microstructure Development', *Journal of the American Ceramic Society*, pp. 3–21.
[27] Bentz, D. P. (2007) 'Cement hydration: building bridges and dams at the microstructure level', *Materials and Structures*, 40(4), pp. 397–404.
[28] Ye, G., van Breugel, K. and a.L.a. Fraaij (2003) 'Three-dimensional microstructure analysis of numerically simulated cementitious materials', *Cement and Concrete Research*,

559 33(2), pp. 215–222.
560 [29] Bishnoi, S., Joseph, S. and Kaur, A. (2018) 'Microstructural modelling of the strength
561 of mortars containing fly ash using μic', *Construction and Building Materials*. Elsevier
562 Ltd, 163, pp. 912–920.
563 [30] Wong, H. H. C. and Kwan, a. K. H. (2008) 'Packing density of cementitious materials:
564 measurement and modelling', *Magazine of Concrete Research*, 60(3), pp. 165–175.
565 [31] Wong, H. H. C. and Kwan, A. K. H. (2007) 'Packing density of cementitious materials:
566 part 1—measurement using a wet packing method', *Materials and Structures*, 41(4), pp.
567 689–701.
568 [32] Wang, M. and Al-Tabbaa, A.(2014)' Computer simulation of the packing of digitized
569 reactive magnesia particles'. *Proceeding of the RILEM International Symposium on*
570 *Concrete Modelling 2014* (pp.36-43). Tsinghua University, Beijing.
571 [33] Wang, M. and Al-Tabbaa, A.(2015) 'Computer simulations of the hydration-
572 carbonation processes in reactive magnesia cement systems.' *5th International Conference*
573 *on Accelerated Carbonation for Environmental and Material Engineering.Columbia*
574 *University*, New York.
575 [34] Vu-Quoc, L., Zhang, X. and Lesburg, L. (2000) 'A Normal Force-Displacement Model
576 for Contacting Spheres Accounting for Plastic Deformation: Force-Driven Formulation',
577 *Journal of Applied Mechanics*, 67(2), p. 363.
578 [35] Vu-Quoc, L., Zhang, X. and Lesburg, L. (2001) 'Normal and tangential force–
579 displacement relations for frictional elasto-plastic contact of spheres', *International*
580 *journal of solids and structures*, 38, pp. 6455–6489.
581 [36] Zhang, M., Ye, G. and Van Breugel, K. (2012) 'Modeling of ionic diffusivity in non-
582 saturated cement-based materials using lattice Boltzmann method', *Cement and Concrete*
583 *Research*. Elsevier Ltd, 42(11), pp. 1524–1533.
584 [37] Gitman, I. M., Gitman, M. B. and Askes, H. (2006) 'Quantification of stochastically
585 stable representative volumes for random heterogeneous materials', *Archive of Applied*
586 *Mechanics*, 75, pp. 79–92. doi: 10.1007/s00419-005-0411-8.
587 [38] Zhang, M. (2013) Multiscale Lattice Boltzman-Finite Element Modelling of Transport
588 Properties in Cement-based Materials. Figure 5.17. Thechnische University Delft.
589 [39] Farrell, G. R., Martini, K. M. and Menon, N. (2010) 'Loose packings of frictional
590 spheres', *Soft Matter*, 6(13), p. 2925. doi: 10.1039/c0sm00038h.
591 [40] Breugel, K. Van (1991) Simulation of hydration and formation of structure in
592 hardening cement-based materials. Phd thesis. Delft University Press.
593 [41] M. Wang (2017) Numerical modelling of the kinetics and microstructural development
594 of carbonated magnesia-based cements. Phd thesis. University of Cambridge.